Chapter 5

5.0 EXPERIMENT 2

TITLE: FLUORESCENCE IMAGING OF MOUSE OOCYTES

5.1 ABSTRACT

This chapter has been is divided into four experimental parts. The main aims were to characterise maturation stages and factors affecting mouse oocyte competency by examining selected structural development using ICC staining. The factors included were maturation conditions, duration of incubation, oocyte retrieval times of the day and zona dissection (PZD). Structures detected were NM, MS, CG and actin filaments. Nuclear maturation was assessed through the activities of the nuclear materials and meiotic spindles arrangement and cytoplasmic maturation using cortical granules distribution. Factors involved in producing high yields of MII oocytes vary depending on strains and culture conditions. The production of MII oocytes of ICR mice were significantly higher in *in vitro* than *in vivo* condition. However, its CG appearance was low. This suggests activation of oocytes in *in vitro* environment that caused loss of CG through exocytosis. Low MS was also observed among F_1 mice during 6 hours of *in vitro* maturation as compared with 3 hours. Such reduction was not observed in C57BL/6J oocytes. Nevertheless, collecting oocytes at 1200 hours of the day improved MII oocytes by two-folds in both strains during both *in vivo* and *in vitro* conditions than at 0900 hours. This was also manifested by high correlation values between MII oocytes with structural appearances under study. The C57BL/6J oocytes were further shown to have higher structural formation under PZD treatment but not F_1. In conclusions, the interplay of various factors including strains, culture conditions and post-hCG time of oocyte retrieval would determine maturation stages and structural distributions in the mouse oocytes.

Keywords: Fluorescence imaging, MI oocyte, MII oocyte, oocyte maturation, oocyte competency.

5.2 INTRODUCTION

The morphology of mammalian oocytes including murine species have been extensively reported in the literature as listed in Table 5.1. Assessment of good quality oocytes is generally made based on its morphological appearances through microscopic observation which could be enhanced by using various imaging devices and softwares (Vonesh *et al*., 2006). The assessment has many significant implications especially for *in vitro* applications of the oocytes such as IVF, nuclear transfer, embryonic stem cells production, gene manipulation and oocyte manipulation. Good oocytes are categorised with a small peri-vitelline space and a regular and distinct first polar body (Suppinyopong *et al*., 2000). The above-mentioned criteria are usually associated with increased pregnancy (Ebner *et al*., 1999). The morphological scoring of good oocytes for IVF application is mainly determined by using microscopic imaging such as Differential Interference Contrast (DIC) and Hoffman Modulation Contrast (HMC). However, oocyte intracellular structures could only be determined by using staining methods. The conventional staining techniques commonly used are Giemsa stain for DNA materials (Tateno and Kamiguchi, 2007) and Coomasie stain for the cytoskeleton (Navarro-Garcia *et al*., 1999). Nowadays, fluorescence staining is widely adopted by many laboratories to reveal the details of internal architectures of mammalian oocytes (Schatten *et al*., 1985, 1993; Hewitson, 1995; Abbot *et al*., 1998) for obtaining a better understanding not only on the complexity of its structural development but also the important mechanisms associated with cellular processes. Some other criteria reported for grading of oocytes included cytoplasmic appearance and granular structures (Daniel, 1971), changes in the organisation of the

plasma membrane and microtubular morphology (Elder and Dale, 2000). These were reported to play an important role in the acquisition of oocyte meiotic competence.

The fertilising capability of oocyte is determined mainly by their maturation stage. Most mammalian eggs are meiotically arrested at dictyate stage of prophase I and resume cell cycle progression to metaphase II (MII) only hours before ovulation. Hormonally induced animals may take 10 to 13 hours for ovulation to occur (Daniel, 1971) and subsequently mature. The rate at which an oocyte attains maturity varies and can be affected by multitude of factors which include age, nutrients, strains, health, environmental stress and oestrus stage. A mature oocyte is usually marked by the presence of polar body. In contrast to the natural process, maturation stages of oocyte *in vitro* is influenced by various factors such as the hormones used, the time at which hormones were injected, retrieval time, the site from which oocytes were retrieved and also compositions of the culture medium used. Oocytes directly retrieved from the follicles or even from the oviducts may be of different maturation stages; germinal vesicles (GV), MI phase and MII phase oocytes.

Two crucial processes of oocyte maturation include nuclear maturation and cytoplasmic maturation. Grondahl (2008) has defined oocyte nuclear maturation as modifications that take place during resumption of meiosis, producing a haploid chromosome complement from the diploid state. He defined cytoplasmic maturation as the unity of processes modifying the oocyte cytoplasm that are essential for fertilisation and pre-implantation embryonic developmental competence. Nuclear maturation is essentially required for fertilisation to take place. Nevertheless, cytoplasmic maturation is equally important for cleavage and subsequent embryonic development *in vitro* and seems to be independent of the nuclear division cycle (Elder and Dale, 2000). Cytoplasmic maturation

requires relocation of organelles and establishment of oocyte polarity, with an increase in the number of mitochondria and ribosomes to support protein synthesis. The cytoplasmic components of oocyte that are required to support early fertilisation include yolk granules, pigment granules, mitochondria, cortical granules and a layer of membrane bound vesicles located beneath the plasma membrane. Membrane bound vesicles of the cytoplasm include crystalline bodies, fat droplets and glycogen granules. One peculiarity of the mouse oocytes is the lack of centrioles (Brunet *et al*., 1999) and another is that oocytes which failed to reach 60 μm would never developed *in vitro* (Epigg and Shcroeder, 1989). Also, the frequency of premature metaphase I arrest decreased markedly as the age of the mice and oocyte volume increased (Sorenson and Wassarman, 1976).

Many aspects of cellular and molecular developments of mouse oocytes need to be studied and analysed during *in vitro* maturation (IVM) in contrast to its *in vivo* maturation (IVO). There were factors reported to influence oocyte maturation including culture conditions and strains (Ibanez *et al*., 2005). *In vivo* produced oocytes are generally of superior quality with respect to production of healthy embryos and offspring. It is well documented that nuclear maturation usually occurred among the *in vitro* matured oocytes but complete cytoplasmic maturation is not really assured (Epigg *et al*., 1996). Liu *et al*. (2005) also reported that tempos of nuclear maturation and cortical granules redistribution were slower among *in vitro* than the *in vivo* matured oocytes.

Resumption of meiosis, also known as oocyte maturation is a crucial manifestation of most mammalian egg development during which the oocyte would go through complex changes; they grow and switch many genes on or off in preparation for the development. These series of complex biological processes that the oocyte must go through in reaching maturity states is also called meiotic maturation (Schultz *et al*., 1989). In mouse oocytes,

the first meiotic M-phase is very long; lasting from 6 to 11 hours, depending on the genetic background (Brunet *et al*., 1999). The earliest morphological changes which occured during maturation process is the breakdown of nuclear membrane or germinal vesicle breakdown (GVBD), at which transcription of new RNA stops almost completely (Elder and Dale, 2000). The progressive aggregation of numerous microtubule organising centres (MTOC) forms the spindle poles, and a bipolar spindle is present during most of the first meiotic M-phase (Brunet *et al*., 1999). This is followed by the formation of meiotic spindle and the move of chromosomes to the periphery of the cell. The first meiotic division separates homologous chromosomes. Also, cortical granules are redistributed as the cell size increases to 100 μm in diameter. At this stage, one set of homologous chromosomes is surrounded by a small amount of cytoplasm. This structure extrudes as the first polar body and then arrested (Hogan *et al*., 1986). Polarisation is obvious at this stage of mouse oocyte development, whereby a microvillus free area on the plasma membrane, adjacent to the polar body overlying the meiotic spindle mark the animal pole of the oocyte. This stage is also known as metaphase II stage oocyte, which is relatively quiet cell, with a pre-set developmental programme.

In response to the preovulatory surge of LH, MII oocytes are expelled into the infundibulum of the oviduct waiting to be fertilised by sperm. Eggs ovulated from the follicles of mouse ovaries accumulated in the distal part of the oviducts called ampullae and are surrounded by sticky mass cells called cumulus cell complex. These granulosa derived cells communicate with an oocyte through gap junction. The arrest at MII stage of a mature oocyte is maintained by maturation promoting factor (MPF) (Kono *et al*., 1995) and the two components of the factor (MPF) identified are tyrosine kinases and cyclin B2, which oscillate with meiotic cycles: increases during GVBD, remains high at MI,

disappears transiently at the time of first polar body extrusion, reappears at MII, and remains elevated level until fertilisation. These components are stabilised by cytostatic factor (CSF) that contained c-mos proto-oncogene product; protein that is responsible for MPF activation. In mouse oocyte, this factor is only necessary for metaphase arrest at meiosis II before fertilisation (Elder and Dale, 2000). Mos protein that is the activator of MAP kinase (mitogen associated protein kinase) not only preventing the oocyte from entering interphase between metaphase I and metaphase II but also maintaining chromosomes condensation, reorganisation of microtubules, spindle formation at metaphase I, stabilisation of the spindle at metaphase II, and therefore mediates as spindle assembly checkpoint (Elder and Dale, 2000). In addition, Kubiak *et al.* (1993) suggested that the mechanism maintaining the metaphase arrest in mouse oocyte involves the equilibrium between cyclin synthesis and degradation, probably controlled by CSF and which is also dependent upon the three dimensional organisation of the spindle. Thus, progression beyond metaphase II requires destruction of MPF activity, which is stimulated by calcium-mediated activation of calcium dependent protein kinase II (Kono *et al*., 1995). It is noted generally, oocyte maturation to MII stage appears to be slower in *in vitro* follicle culture as compared with *in vivo* maturation (Hu *et al*., 2001; Liu *et al*., 2005). Prolonging culture of oocytes past 16 hours post-hCG may further increase the yield of oocyte in MII. However, ageing of oocytes at MII may cause concomitantly a deterioration of the spindle and displacement of chromosomes from the spindle equator.

Recent molecular study showed that among the many substances to influence oocyte maturation is the endogenous signaling molecule; FF-MAS (4,4-dimethyl-5α cholest-8,14,24-trien-3β-ol), an intermediate in the cholesterol biosynthetic pathway present in cells (Byskov *et al*., 1995). This substance has triggered the resumption of

meiosis (nuclear maturation) of mouse oocyte *in vitro* (Grondahl *et al*., 1998). It is also capable of initiating meiosis in isolated naked or cumulus cell-enclosed oocytes from several species (Byskov *et al*., 1995). Another study showed that the formation of polar body, asymmetrical organisation of meiotic spindles and arrangement of chromosmes at the oocyte cortex in mice was associated with protein formis (Liu *et al*., 2003). Meanwhile, in bovine, administration of cAMP in culture medium showed that granulosa cumulus oocyte complexes (GCOCs) remained at prophase I with intact germinal vesicle but germinal vesicle breakdown was observed among the cumulus oocyte complexes (COCs). Nonetheless, both groups of oocytes were reported to resume meiotic division in hormone and serum free medium (Aktas *et al*., 2003). In contrary, the recent finding reported that a higher capability of cortical granules release was observed among oocyte matured in the presence of serum than those matured without the serum (Ibanez *et al*., 2005). Also, Liu *et al*. (2005) reaffirmed that the presence of serum in maturation media enhanced cortical granules release after aging or activation of oocytes.

The cytoplasm of the mammalian oocytes consists of complex matrix of cytoskeletal elements, including actin, tubulin and certain cytokeratins (Hogan *et al*., 1986). The monomeric proteins that comprise microtubules are α and β tubulins. The γ tubulin, a third tubulin protein is not present in microtubules, but is thought to nucleate the initial polymerisation of α and β tubulins. Tubulin filaments are mostly found in the cytoskeleton and meiotic spindles of an oocyte. Gobarsky *et al*. (1990) injected biotinylated tubulin into living oocyte that was subsequently incorporated into the meiotic spindle and found that this component of the microtubules within the arrested metaphase spindle of the mouse oocyte undergo rapid cycles of assembly and disassembly. Microtubules of the telophase midbody are more stable. These spindle shaped microtubules that partition chromosomes

are classified as short lived structures. They appear after interphase and disappear after mitosis is completed. Although microtubules in a cell may seem to be arranged in a somewhat random pattern, in fact, they are usually in a hub and spoke formation with the hub near the centre of the cell. This hub is called the centrosome and is the primary microtubules organising center (MTOC) of the cell. Polymerisation of microtubules is temperature dependent. At low temperatures, microtubules tend to depolymerise, whereas at higher temperatures, they spontaneously polymerise. Above a critical concentration polymerisation is favoured and vice versa. During polymerisation, microtubules radiate outward with the +ve ends moving away from the centrosomes.

The role of cytoskeletal microtubules and microfilaments in the process of egg maturation and fertilisation in various kinds of mammalian oocytes has been reported in the last decade. In *Xenopus* egg, interactions between individual cytoskeletal components and internal membranes are important for organisation of the cortex and cortical actin is required for anchoring and rotation of the meiotic spindle. It has also been suggested that the first contact of mammalian sperm with an oocyte involves an early reorganisation of the oocyte cytoskeleton. Clusters of mouse oocyte chromosomes are redistributed around the cortex in a microfilament dependent process (Veselska and Janish, 2001). The system has been reported to coordinate the migration of maternal and paternal pronuclei when sperm fertilised an oocyte. Microtubules forming within the mouse egg during fertilisation are required for the movements leading to the union of the sperm and egg nuclei. In an unfertilised oocyte, microtubules are predominantly found in the arrested meiotic spindles. At the time for sperm incorporation, a dozen cytoplasmic asters assemble, often associated with the pronuclei formation (Schatten *et al*., 1985). They also reported that meiotic spindle of unfertilised oocyte is anastral, barrel shaped, and attached to the oocyte cortex

and probably interact with the perinuclear actin found in pronucleate eggs. It has been postulated that the activity of MPF: histone H1 phosphorylation not only contribute to chromosome condensation and nucleosome packing alteration but also rearrangement of microfilament, reorganisation of intermediate filament network, and nuclear disassembly. Hu *et al*. (2001) also reported that spindle morphology and chromosome alignment can be used as one indicator of the oocyte's capacity to form chromosomally balanced embryo. In mice, mirotubules in the pronucleate stage zygote are organised as multiple cytoasters instead of the expected single sperm aster. Furthermore, centrosomal material is detected in unfertilised oocyte but not in the sperm (Navara *et al*., 1994; Schatten, 1994; Schatten *et al*., 1986). Schatten *et al*. (1991) had conducted studies involving parthenogenesis, polyspermy and recovery from microtubule inhibitors to support the hypothesis that the mouse centrosome is of maternal origin. The evolutionary shift from paternal to maternal centrosomes in mice is probably due to their short generation time in which the females are sexually mature around 1.5 months versus the 1.5 decade norm of humans (Schatten, 1994). It has been proven that in murine oocyte development, microfilaments are crucial for cortical meiotic spindle positioning and maintenance, formation of the first and second polar bodies, incorporation of cone formation, pronuclear apposition, and cytokinesis. Nevertheless, actin assembly is not required for sperm head penetration in the mouse (Simerly *et al*., 1998). In addition, the earliest developmental changes in actin organisation in the egg are seen at fertilisation. In the ovulated oocytes the plasma membrane above the meiotic spindle is devoid of concanavalin A (Con A) binding sites and microvilli, and is underlaid by actin rich subcortical layer. Fertilisation results in the formation of a second Con A free zone, the fertilisation zone, which is around the site of sperm entry. The plasma membrane of this region is also underlaid by an actin rich layer. As the pronuclei move

toward the centre of the egg, the distribution of actin filaments become more uniform and the Con A free regions disappear. The microfilaments of human oocytes formed a very fine meshwork localised particularly in the cortical region. Individual fibres either extended into remnants of the zona pellucida or, occasionally, formed cell surface protrusion called microspikes or microvilli. The bundles of microfilaments in a mouse oocyte were thicker as compared with the actin filaments in human oocyte (Veselska and Janish, 2001). Actin structures are also involved in the process of meiotic division I and extrusion of first polar body. It has also been confirmed that the migration of cortical granules is driven by microfilaments and not by microtubules. Anchorage of cortical granules to the cortex is independent of these cytoskeletal structures. Neither microtubules nor microfilaments are involved in exocytosis of cortical granules (Veselska and Janish, 2001). It has been reported that at 2 hours, fertilised MII mouse eggs underwent a mean CG loss of 69% and the entire cortex occupied by CG but not in the fertilised GVBD and the prometaphase I. The mechanism of propagating a normal wave of CG loss from the site of sperm entry develops between MI and MII oocyte (Ducibella and Buetow, 1994).

The ICC technique utilised in this study had revealed some of the structural abnormalities that may have contributed to the failure of meiotic completion and the search for superior eggs suitable for cultivation continues. Some of the past studies on the morphology of mammalian oocytes are shown in Chapter 4 (Table 4.1) and described in chronological order in Table 5.1. In brief, Downs *et al*. (1986) revealed that *in vitro* maturation of mouse oocytes can be inhibited simultaneously by adding hypoxanthine and adenosine into the incubation medium. Hypoxanthine also blocked GVBD, postponed cortical granules migration and prevented cortical granules free domain formation (Liu *et al*., 2005). Meanwhile, the metaphase plate of MI stage in bovine oocyte occurred by 6.6

hours of culture following GVBD (De Loos *et al*., 1994). Another study conducted by Sirad and Blondin (1996), reported that different developmental potential was observed between IVO and IVM bovine oocytes. However, the groups displayed similar rates of nuclear maturation, fertilisation and cleavage formation. Retardation of spontaneous cell cycle progression and meiotic competence in mouse oocytes cultured *in vitro* was detected by using DAPI to stain the nuclear materials and LCA-biotin texas red to detect blockage of cortical granules exocytosis (Abbot *et al*., 1998). A study on porcine oocytes showed that cooling can cause irreversible damage of both the chromosome and meiotic spindle (Leader *et al*., 2002).

Mouse oocyte has been claimed to be the excellent model for exploring microtubular fibres such as myosin structure and function (Lee *et al*., 2000). It has also been reported that immature germinal stage oocyte matures spontaneously *in vitro* and can be arrested at specific cell cycle during first meiosis. This permits observations on dynamic motility events such as peripheral spindle migration, cortical spindle anchoring, and cell surface modification (Lee *et al*., 2000). Ovulated oocyte is arrested at metaphase of the second meiosis and can be artificially activated or fertilised *in vitro*, permitting detailed investigations on spindle rotation and cytokinesis during second polar body formation and the event during sperm incorporation, pronuclear formation, and migration, as well as mitosis, can be investigated.

5.3 OBJECTIVES

The aims of this study were, a) to reveal the general architectures of the *in vivo* and *in vitro* matured oocytes in different strains of mice by using fluorescence imaging, b) to study the effects of retrieval hours post-hCG injection on oocyte structures and c) to evaluate the effect of micromanipulation such as partial zona dissection on the oocyte structures.

Table 5.1: Timeline on some of the significance findings on cellular architectures of mammalian oocytes

Year	Author	Species	Description
1986	Downs *et al*.	Mouse	The simultaneous addition of hypoxanthine and adenosine into the incubation medium inhibits *in vitro* maturation of mouse oocyte
1994	De Loos *et al*.	Cattle	GVBD occurs within hours after removal from the follicle or the ovulatory LH signal. By 6.6 hours of culture, approximately 50% of the oocyte undergone GVBD. Then, the chromosomes condensed further. The kinetochores appear and the microtubules pull the chromosomes and they form the metaphasic plate of MI.
1996	Sirard and Blondin	Cattle	Oocyte matured *in vitro* or *in vivo* have similar rates of nuclear maturation, fertilization and cleavage, but clearly differ in their developmental potential
1998	Abbott *et al*.	Mouse	*In vitro* culture retards spontaneous cell cycle progression and the meiotic status was determined by DNA staining using DAPI. Cortical granule exocytosis was disrupted too and this was detected by using *Lens culinaris* –biotin-Texas red
2002	Leader *et al*.	Pig	Cooling caused non-reversible damage of both chromosomes and meiotic spindle.
2003	Liu *et al*.	Mouse	Formis (FH proteins) is associated with the formation of polar body and also organisation of asymmetry spindle and arrangement of chromosomes at the oocyte cortex.
2003	Aktas *et al*.	Cattle	Regulation of meiotic state in granulose cumulus complex oocyte (GCOC) and cumulus oocyte complex (COC) with cAMP showed GCOC remained at prophase with intact germinal vesicle (GV) but COC underwent germinal breakdown (GVBD) but in hormone and serum free medium they resume meiosis.
2005	Ibanez *et al*.	Mouse	Strains and culture condition affect nuclear and cytoplasmic maturations in mouse oocyte.
2008	Grondahl	Horse, pig	Addition of FF-MAS to the maturation medium improves the cytoplasmic maturation and yields higher quality pre-embryos.

5.4 SIGNIFICANCE OF THE STUDY

Determining oocyte morphology using fluorescence staining could reveal intracellular architectural dynamics which are directly or indirectly related to oocyte developmental competence. Some of the structures such as cytoskeleton are generally not clearly revealed through conventional staining that consequently lead to uncertainties on specific morphological development at different maturation stages of oocytes. Determining oocyte developmental competence between strains and culture conditions enables ones to identify suitable criteria to be included for cultivating high quality oocytes, consequently improving fertilisation rate and subsequent embryonic development *in vivo* and *in vitro*. Also, the study may reveal more information on architectural development of *in vivo* and *in vitro* matured oocytes and variation that occur between strains. In other words, by comparing oocyte architectural topography, susceptibility of different strains of mouse oocytes towards *in vivo* and *in vitro* environment especially during micromanipulation could be assessed and compared. Thus, their further survival and developmental competence can be predicted.

5.5 MATERIALS

The materials required in this study were as described in Sections 3.3, 3.4, 3.5 and 3.6. In brief, female mice from the following strains which were ICR, C57BL/6J and F_1 hybrids of CBA×C57BL/CJ were used and sacrificed at the age between 8-10 weeks old. Superovulation through PMSG and hCG admininstrations was described in Section 3.3.3. The TYH medium and hyaluronidase acid (HA, 0.1%) were used to prepare naked oocytes. Zona dissolution was conducted using acid Tyrode's solution (pH 2) and zona dissection method followed Nakagata (2000) with modifications. Washing and rinsing of the oocytes

were conducted in sodium hepes-containing medium (HWM). The fluorescent dyes were as listed in Section 3.6.3.3.1.

5.6 PROCEDURES

The experiments were divided into four parts. The procedures for each part were described in the following subsections.

5.6.1 Fluorescence Imaging of Mouse Oocyte *In Vivo* and *In Vitro*

Female mice of three different strains, which were ICR, C57/6J, and F_1 (CBAxC57/6J), were superovulated with PMSG and hCG, 5 IU of each, 48 hours apart. They were sacrificed 13 hours later and the oocytes were processed for fluorescence staining and imaging. Prepared oocytes were eventually stained for detecting its microtubules, cortical granules and the nuclear materials. Some of the oocytes were further incubated in TYH medium inside the CO_2 incubator for 3 to 5 hours before they were finally prepared for fluorescence staining. The oocyte preparation and staining procedures were as described in Sections 3.4.5 and 3.6.3.6, respectively.

5.6.2 Effect of Post-hCG Retrieval Time on Ooocyte Morphology in Different Culture Conditions

Following hCG injection, superovulated female mice of F_1 hybrids were sacrificed next day at two different times, which were 900 to 1100 hours and 1200 to1400 hours. The *in vivo* group was immediately stained, while the *in vitro* group was matured further in *in vitro* condition for another two to three hours. The morphology of the oocyte was compared by studying the nuclear materials, the meiotic spindle and the cortical granules.

5.6.3 Effect of *In Vitro* Incubation Hours on Mouse Oocytes

5.6.4 Effect of Zona Dissection on Mouse Oocytes

Oocytes retrieved from female mice were exposed to *in vitro* culture for three hours following zona dissolution and zona dissection. The procedure for zona dissection followed Nakagata (2000) as briefly described in Section 3.5.5.3. The oocytes were then prepared for fluorescence staining (Section 3.6.3.6.5) and observed under the fluorescent microscope.

5.7 MICROSCOPIC OBSERVATION

All stained oocytes were examined under the Nikon Ohptiphot UFX fluorescent microscope and the Carl Zeiss inverted fluorescent microscope. Most of the images were captured at 400x magnification using Nikon camera loaded with Kodak film which were then processed and edited using Photoshop editor for colour tones and sharpness. Some observations were digitally recorded using cooled CCD camera linked to Pro-plus image editing software.

5.8 EXPERIMENTAL DESIGN

The summary of experimental design is shown in Table 5.2. In the first part, three criteria of oocyte morphology namely MS, MTOC and CG were compared among three different strains of mice in two culture conditions. The second part included F_1 females only, due to its availability when the experiment was conducted. In this part, oocytes were retrieved at two different hours and their morphological differences were compared. Further analysis was conducted to study the effects of incubation hours on IVM oocytes. Two strains which were F_1 and C57BL/6J were included and oocytes were incubated at two incubation hours.

In the third part, the intactness of the aforementioned structures were also analysed among the PZD oocytes as compared with the control group.

Table 5.2: Summary of experimental design of the study with results interpreted as percentages of intact versus aberrant structures

Part of experiment	Category	Dependent variable
Part 1	Maturation condition (2): *in vivo*, i*n vitro* Strain (3): F_1, ICR, C57BL/6J	
Part 2	Post-hCG retrieval times (2): 0900-1100, 1200-1500 hours Culture conditions (2): *in vivo*, i*n vitro* Strain (1): F_1 Incubation hours (2): 3-4 hours, 5-6 hours Strain (2): F_1, C57BL/6J	-Maturation stages, -General morphology -Intactness of meiotic spindles, nuclear materials, cortical granules, actin and MTOC
Part 3	Partial zona dissection (2): PZD vs. IVM Strain (3): F_1, ICR, C57BL/6J	
Experimental	factorials:	
Part 1: 3 x 2,	Part 2: 2 x 2, Part 3: 2 x 2,	Part 4: 2 x 3

5.9 STATISTICAL ANALYSIS

Data was quantitatively analysed using SPSS Statistical Package and the means between treatments were compared by using One Way Analysis of Variance (ANOVA) followed by Duncan's multiple range test. The significant difference was accepted at significant level $p<0.05$. Results are expressed as percentage of means ± standard error of means (SEM) and correlation test was also conducted in order to determine relationships between the structures under study.

5.10 RESULTS

The results of each experiment are grouped into several sections as follows:

5.10.1 Fluorescence images of *in vivo* and *in vitro* oocytes in different strains of mouse.

5.10.2 Effects of post-hCG retrieval times on oocytes maturation and morphology.

5.10.3 Effects of *in vitro* maturation durations on oocyte structures.

5.10.4 Effects of partial zona dissection on oocyte structures.

5.10.1 Fluorescence Images of *In Vivo* and *In Vitro* Oocytes in Different Strains of Mice

The results are discussed and divided into various sections as the following order.

5.10.1.1 General morphology

The fluorescently stained *in vivo* as well as *in vitro* treated mouse oocytes revealed comparable morphology and polarity for the architectures and distributions of the meiotic spindles, cortical granules and the nuclear materials between strains. Fluorescence staining clearly distinguished the animal from the vegetal pole (Figure 5.1), which was usually inconspicuously observed under the conventional bright field microscope, unless the vesicular structures were found, aggregated at the vegetal pole as shown in Figure 5.2. In Figure 5.1, eccentric location of cortical granules (Figure 5.1b, red), meiotic spindle (Figure 5.1c, yellowish green) and the nuclear materials (Figure 5.1d, blue) were clearly shown as compared with the oocyte's corresponding image obtained from the bright field image (Figure 5.1a). Little information could be extracted from the bright field image. However, in certain circumstances, the nuclear materials and the meiotic spindles that were fixed in formaldehyde solution could be traced under the bright field microscope. The structures then were reaffirmed and clearly visualised under the fluorescent light (Figures 5.3).

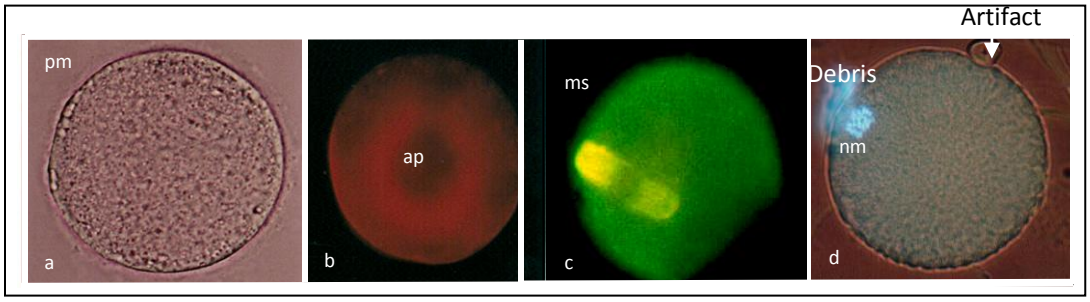

Figure 5.1: Comparative images between the bright-field and fluorescently stained oocytes. (a) Bright-field image of MI oocyte, (b) the corresponding oocyte stained with TRITC-LCA, (c) meiotic spindles, (d) composite image of bright-field and nuclear materials stained with Hoechst. ap-animal pole, ms-meiotic spindle, nm-nuclear materials, pm-plasma membrane. (400x)

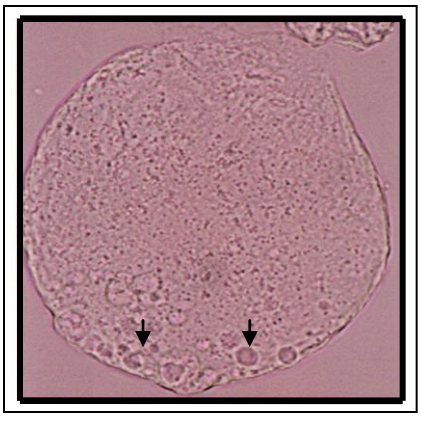

Figure 5.2: Bright-field image. Arrows showing granular vesicles at the vegetal pole of the oocyte. (400x)

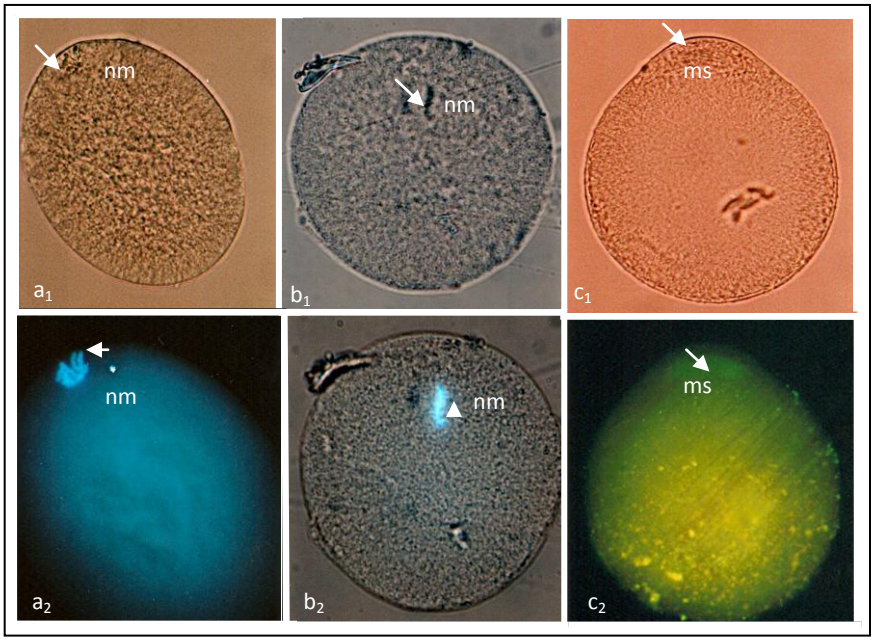

Figure 5.3: Top: Bright-field images of MI oocyte. (a_1), (b_1) arrows showing the nuclear materials, (c_1) arrow showing meiotic spindles. Bottom: Fluorescence images of the corresponding structures. (a_2), (b_2) arrows showing the nuclear materials that were stained with Hoechst, (c_2) the meiotic spindle (arrow) that was stained with FITC. ms-meiotic spindle, nm-nuclear materials. (400x)

Shape of oocytes was not strain-specific too. Images showed that most of the oocytes were of round shape, while others appeared oval, potato shape, egg-shape and irregular round shape. One of the contributing factors for such variations could be due to how they were placed and positioned onto the coverslips or the glass slides. The shape of an oocyte could also be used as the indicative criterion for determining the oocyte poles. Although, it might not be always applicable to all oocytes, nevertheless, for most of the

oval shaped and egg shaped oocytes the broader end was the vegetal pole and the opposite, narrower end was the animal pole. The later was where the nuclear materials and the meiotic spindle were located. Under the fluorescent microscope, the animal pole of MI oocyte appeared as empty space that was devoid of cellular materials when stained with TRITC-LCA (Figure 5.4).

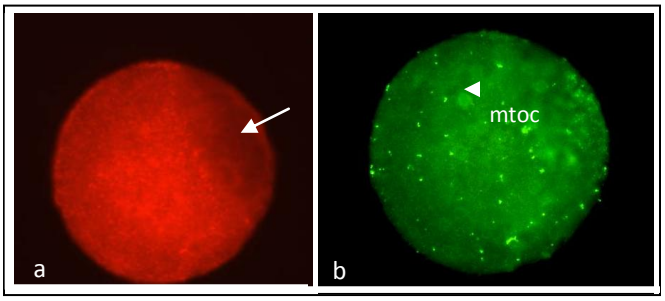

Figure 5.4: (a) MI oocyte stained with TRITC-LCA showing translucence animal pole (arrow) and (b) corresponding oocyte stained with FITC showing MTOC. mtoc-microtubule organising centre. (400x)

Polarity of the MII oocyte was also indicated by the presence of a polar body resulting from the second meiotic division. The nuclear materials and the spindles were easily detected under both the bright field and fluorescent microscopes (Figure 5.5).

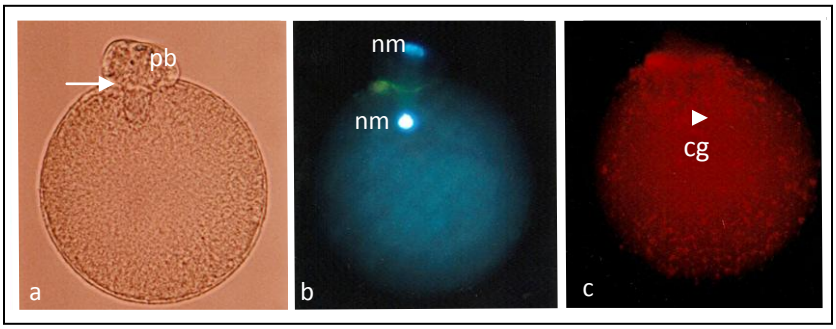

Figure 5.5: Images of MII oocyte fixed in formaldehyde solution. (a) The bright field image showing meiotic spindles (arrow), (b) corresponding image stained with Hoechst showing telophase I stage and (c) TRITC-LCA image. cg-cortical granules, nm-nuclear materials, pb-polar body. (400x)

In general, most of the oocytes displayed their nuclear materials and the meiotic spindles at the periphery of the animal pole while cortical granules were abundance either at the centre or at the bottom hemisphere towards the vegetal pole. The spindles of the MI and MII oocytes were arranged and positioned differently. In MI oocytes the meiotic spindles extended in tangential position but radial or vertical arrangement for the MII oocytes. The meiotic spindles among the MI oocytes might be less indicative of the maturation stage because its position is also determined by the angle at which an oocyte was attached onto the coverslips. However, staining had revealed various stages of nuclear and cytoplasmic maturation among the *in vivo* and *in vitro* oocytes. In Figures 5.6, 5.7, 5.8 and 5.9 archives of fluorescence images of the MI and MII oocytes obtained from the different strains of mice were shown. Figure 5.6 shows various arrangements and angles of the meiotic spindles in MI oocytes, revealing the metaphase I stage. A few asters were also seen too in Figure 5.6a. In Figure 5.7, the different views of the nuclear materials were displayed representing metaphase I and metaphase II stages, respectively, among the oocytes. For example, 2n set of chromosomes arranged in circular pattern could be observed during the metaphase II stage (Figures 5.7c, 5.7d).

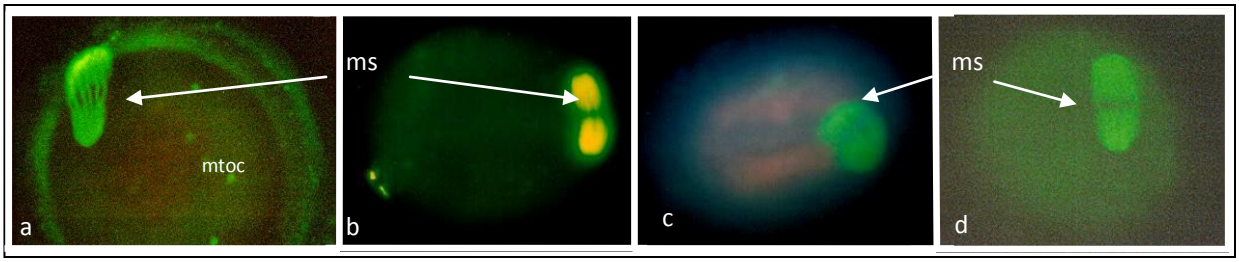

Figure 5.6: Meiotic spindles (MS) of the MI oocytes. (a) Zona-intact oocyte of C57BL/6J, (b) and (c) showing the different shapes and sizes of MS in ICR oocytes and (d) zonaless oocyte of C57BL/6J. ms-meiotic spindle, mtoc-microtubule organising centre. (400x)

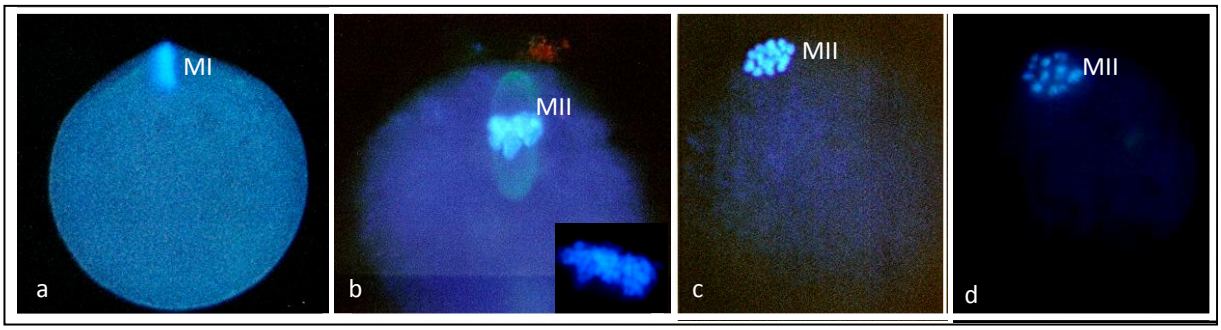

Figure 5.7: Nuclear maturation stages: (a) Metaphase I of F_1 hybrid, (b) MII of C57BL/6J oocyte, (c) MII of F1oocyte and (d) MII of ICR oocytes. Inset of Figure 5.7b shows nuclear materials of MII stage at 1000x magnification.

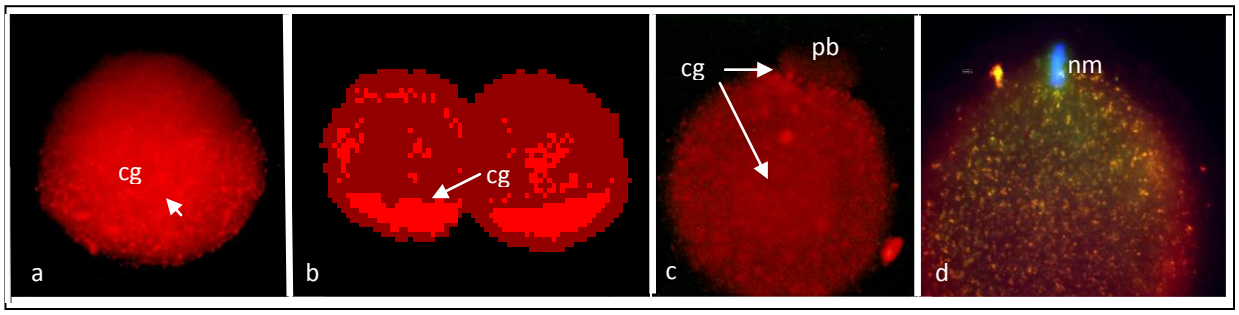

Figure 5.8: Cortical granules (arrows) in MI (a and b) and MII (c) oocytes. (d) Composite of three fluorescent dyes (blue for NM, green for MS and red for CG). cg-cortical granules, pb-polar body, nm-nuclear materials. (400x)

Figure 5.8 reveals the distributions of cortical granules in MI and MII oocytes, respectively. Healthy unfertilised oocytes have CG centrally distributed or aggregated at the vegetal pole meanwhile uneven distribution was observed among the unhealthy ones as shown in Figure 5.8b. As previously reported (Schatten *et al*., 1992), a unique characteristic of murine oocytes was the presence of microtubule organising centre (MTOC) among the unfertilised oocytes. It was observed as small dense round structures with green fluorescence as exhibited in Figures 5.9a, c. The MTOC numbers varied between oocytes and treatments and were found to be distributed at all locations regardless of the poles. Compartmentalisation could be observed in some oocytes as shown in Figure 5.9a. This could be related with organisation of the microfilaments such as actin as shown in Figure 5.10. In Figure 5.10a, actin appeared as a thin layer surrounding an oocyte and it was thicker toward the animal pole especially around the polar body of MII oocyte. Also, actin distribution was observed to be related to smaller compartments of MI oocyte as shown by arrows in Figure 5.10b.

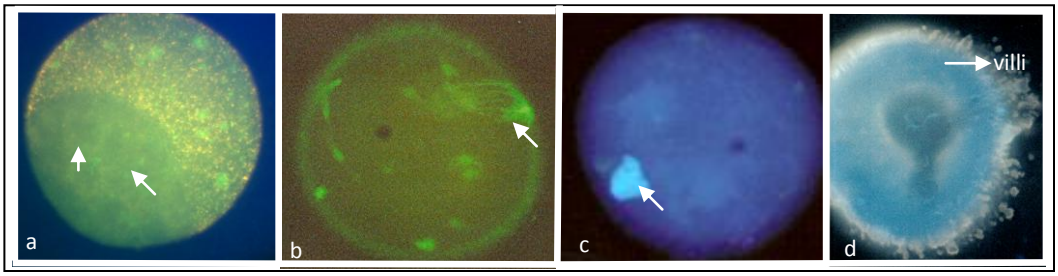

Figure 5.9: Microtubules organising centres (MTOC) in MI oocyte . (a) F_1 oocyte with arrows showing tiny compartments at the animal pole, (b) C57BL/6J oocyte. Arrow showing the meiotic spindles, (c) compacted nuclear materials (arrow) of oocyte, (d) arrow showing villi of oocyte. (400x)

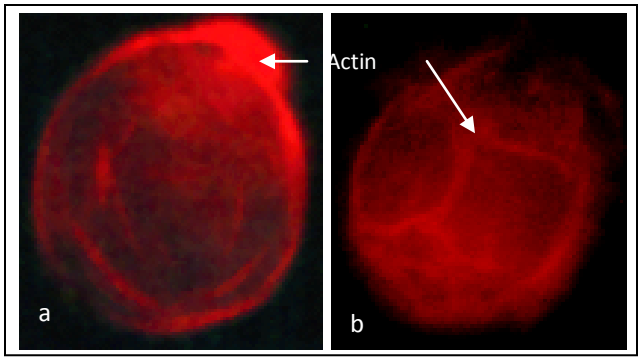

Figure 5.10: Mouse oocyte stained with Alexa-fluor revealing actin microfilaments (red). (a) Arrows showing dense of actin fibres at the animal pole and around the polar body in MII and (b) individual compartment surrounded by actin in MI oocyte. (400x)

5.10.1.2 Maturation and structural appearance of *in vivo* and *in vitro* oocytes

Comparative analysis of maturation stages and structural intactness of oocytes were conducted among strains between different culture conditions. The results were expressed as mean percentages as shown in Tables 5.3 and 5.4, respectively. Intact structures were distinguished from the aberrant counterparts as displayed in Figure 5.11. Misaligned MS (Figure 5.11b_2) and patchy NM (Figure 5.11d_2) were among the most prominent structural abnormalities observed including some oocytes with clear or patchy cytoplasmic granules. From Table 5.3, it was noted that in *in vivo* condition, the mean percentages of MI oocytes were comparable among the strains, which were 67.5±9.8%, 69.2±5.1% and 64.2±19.6%, respectively, for F_1, ICR and C57BL/6J mice. However, low percentages of MII stage were significantly obtained in both IVO and IVM culture conditions. The F_1 mice showed the lowest MII oocytes (6.8±3.4%) *in vitro* as compared with IVO condition (21.2±7.7%). The highest MII value was observed among the ICR oocytes *in vitro*. Contrary to its lowest MI oocytes (56.3±17.8%), ICR mice produced a significantly higher MII stage (47.8±16.5%) *in vitro*. Meanwhile, C57BL/6J showed the highest MII stage (34.8±20.4%) *in vivo* and slightly a lower value (18.6±6.1%) among its IVM oocytes. In general, the results showed that some of the MII oocytes were recorded to have sparsely distributed cortical granules,

aggregation of granular materials at the oocyte circumference, circular arrangement of nuclear materials, darker image at the animal pole which contained mass of condensed nuclear materials and radial arrangement of meiotic spindles (Figure 5 (a-d)).

Table 5.3: Mean percentages of MI and MII oocytes in different maturation conditions

Strain	Maturation condition			
	IVO (%) (Mean±SEM)		IVM (%) (Mean±SEM)	
	MI	MII	MI	MII
F1	67.5± 9.8^{a,y}	21.2±7.7^{a,x}	77.4±10.8^{a,y}	6.8±3.4^{a,x}
ICR	69.2± 5.1^{a,y}	27.3±5.5^{a,x}	56.3±17.8$^{a, x, y}$	47.8±16.5$^{b, x, y}$
C57BL/6J	64.2± 19.6$^{a, y, z}$	34.8± 20.4$^{a, x, y}$	78.8± 8.6$^{a, z}$	18.6± 6.1$^{a, x}$

$^{a, b}$ means within a column in a group differ significantly at $p<0.05$.
$^{x, y, z}$ means within a row in a group differ significantly at $p<0.05$.

The mean percentages of structural occurrences among the cohorts of IVO and IVM matured oocytes between strains were tabulated in Table 5.4. The NM and CG were found to be consistently higher among the IVO and IVM matured oocytes. The highest value for the respective structures was 93.5±3.1% in IVM of C57BL/6J and 98.3±1.7% in IVO of F_1 mice. The highest percentages of MS for both IVM and IVO oocytes were detected in C57BL/6J oocytes with values of 78.5±15.7% and 65.7±16.5%, respectively. These were significantly higher ($p<0.05$) than the MS percentage in IVO oocyte of F_1; the lowest with 23.8±7.9%. However, higher percentage of MS was obtained among its IVM counterpart

with 40.6±8.4%. In addition to MS, the IVM oocytes of C57BL/6J also showed highest percent of NM with value of 93.5±3.9%. This, as well as the percentage of NM in its IVO oocytes were significantly higher ($p<0.05$) than that obtained from IVO of ICR oocytes which was 67.3±11.1%. It was revealed that approximately only 7.5% of MI oocytes of the IVO groups showed nuclear and cytoplasmic degradations. The F_1 oocytes displayed high anomalies of nuclear materials whereas patchy cortical granules were found to be higher in ICR mice. Higher values of degraded nuclear materials were observed among the MI oocytes cultured *in vitro* with approximately 10.3% and 15.7%, respectively, for ICR and C57BL/6J. Approximately 5% patchy cytoplasmic granules were observed among ICR and F_1 oocytes, respectively. The MII oocytes showed that there were approximately 7% patchy nuclear materials and 10% patchy cytoplasmic materials detected among the IVM groups as compared with smaller percentages found among the IVO groups.

Contrary to MS and NM, MTOC structure was comparatively higher among the IVO than the IVM oocytes in all the strains, especially for F_1 oocytes, which differed significantly ($p<0.05$) between the maturation groups. The percentages for its IVO and IVM matured oocytes were 54.8±10.9% and 21.3±7.3%, respectively. Mouse oocytes displayed maternally derived MTOC. It was observed that MTOC numbers ranged between 1 to 33 and 1 to 28, in IVO and IVM oocytes, respectively. However, a majority of the oocytes across the strains produced either 1 or 2 counts of MTOC only and approximately 5% or less showed more than 3 or bigger amount of MTOC per oocyte. Large amount of IVO and IVM produced metaphase I oocytes lacked MTOC. Nonetheless, among those with intact MTOC, the F_1 strain displayed varying amount of the structure ranging from 0-33 *in vivo* and 0-18 *in vitro*. The ICR and C57BL/6J each displayed between 0-19 and 0-23 MTOC, respectively, during *in vivo* condition and a range between

0-28 and 0-15, respectively, during *in vitro* condition. In comparison to MI, the amount of MII oocyte with MTOC structure was higher for both culture conditions and most of them displayed either 1 or 2 MTOC only. In addition to MTOC, the highest percentage of CG appearance was also noted among the IVO oocytes of F_1 with value of 98.3 ±1.7%. Nevertheless, no significant difference was observed among the strains as well as between the maturation groups.

High correlation was determined between selected structures of oocytes. The CG was highly correlated with MS, MTOC and NM in IVO oocytes of F_1 mice, but weak correlations between structures of IVM oocytes. Low correlation values also were found among the structures of IVO oocytes in ICR mice. However, the MTOC structure in its IVM counterparts was highly correlated with NM and MS. On the other hand, the CG of C57BL/6J oocytes was found to correlate strongly with all the structures being studied in both maturation groups. Also, a high correlation was observed between the MS and NM in the IVM oocytes of C57BL/6J.

Table 5.4: Mean percentages of structural occurrences of IVO and IVM oocytes in the different strains of mice

Treatment / Oocyte structures	IVO (%) (Mean ± SEM)			IVM (%) (Mean ± SEM)		
	F_1	ICR	C57BL/6J	F_1	ICR	C57BL/6J
MS	23.8±7.9[a] (n=54)	40.2±14.0 [a,b] (n=57)	65.7±16.5[b] (n=41)	40.6±8.4[a,b] (n=95)	42.7±19.3 [a,b] (n=44)	78.5 ± 15.7[b] (n=48)
MTOC	54.8 ±10.9[a] (n=54)	51.6±5.0[a,b] (n=57)	40.3±8.8[a,b] (n=41)	21.3±7.3[b] (n=95)	45.2±14.9[a,b] (n=44)	30.3 ± 10.7[a,b] (n=48)
NM	89.9±3.3[a,b] (n=83)	67.3±11.1[a] (n=77)	91.3± 5.4[b] (n=53)	79.1±4.0 [a,b] (n=107)	81.9±14.3[a,b] (n=45)	93.5± 3.9[b] (n=72)
CG	98.3±1.7[a] (n=29)	94.2±3.9 [a] (n=46)	80.6±10.0[a] (n=15)	83.6±5.6[a] (n=57)	73.0±13.1[a] (n=27)	80.4±5.4[a] (n=11)

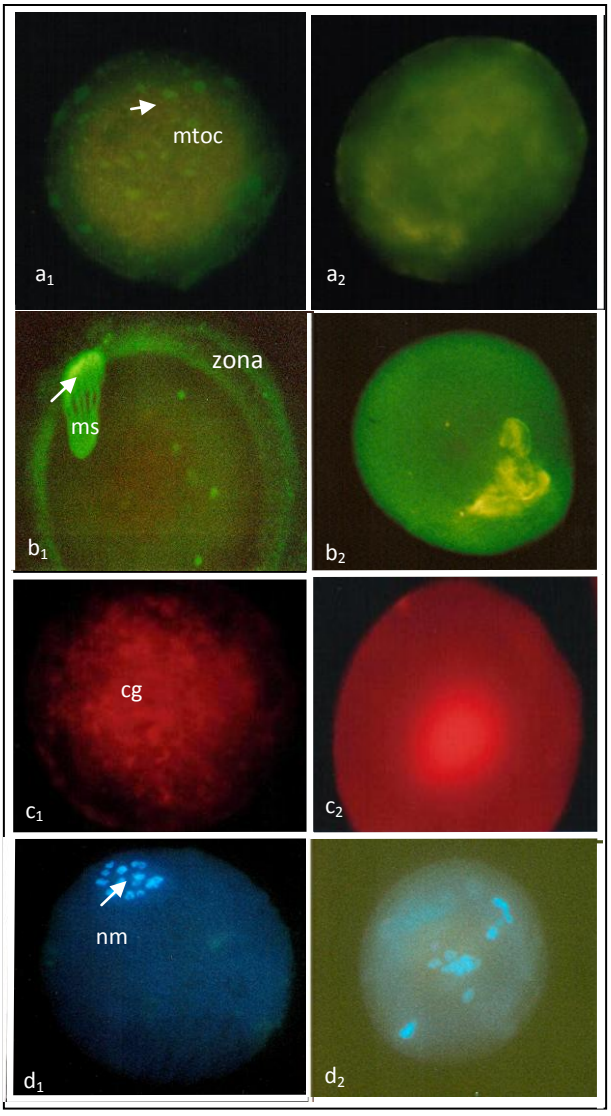

Figure 5.11: Fluorescence images of mouse oocytes showing intact MTOC, MS, CG and NM (a_1-d_1), respectively, and the aberrant counterparts (a_2-d_2). cg-cortical granules, ms-meiotic spindle, mtoc-microtubule organizing centre, nm-nuclear materials (400x)

5.10.2 Effects of Post-hCG Retrieval Times on Oocyte Maturation and Morphology

The results of this part of the experiment were grouped into two sections. The first section compared mean percentages of MI and MII oocytes and the second comprised mean percentages of structural distributions in oocytes at the different times of the day when they were retrieved.

5.10.2.1 Oocyte maturation

Morphological differences between mature and immature oocytes were distinguished mainly by the presence of polar body. A polar body bearing oocyte was categorised as mature of metaphase II stage (MII), while the immature ones were those without the polar body (MI). The fluorescent dye Hoechst revealed the chromosomal activities of the oocyte through which a majority of them were arrested either at the metaphase I or metaphase II stage. A small percentage of anaphase I and telophase I were also detected (Figure 5.12). Apart from chromosomal activities, the orientation of the meiotic spindles was also used to determine the stages among which tangentially positioned spindles marked MI oocyte (Figure 5.12b) as opposed to radial orientation for the MII (Figure 5.7b). Nuclear maturation was assessed through chromosome and meiotic spindles appearances using Hoechst and FITC stains, respectively. The mean values were expressed in percentage as shown in Figure 5.13 and Table 5.5. In this part of experiment only F_1 females were included.

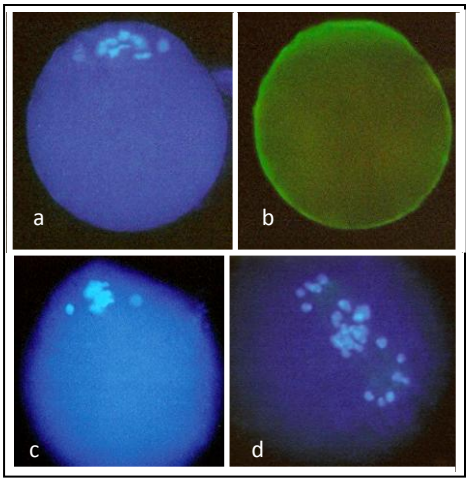

Figure 5.12: Nuclear maturation of oocyte. Anaphase I showing the chromosomes in (a) and (c), and the meiotic spindles in (b). Disorganised separation of chromosomes is shown in (d). (400x)

The means percentages of the MI and MII oocytes varied between the retrieval times post-hCG injection in both groups. The IVM group showed the highest frequency of MI oocytes at 0900-1100 hours and the lowest at 1200-1500 hours of the day. Correspondingly, its low and high values of the MII stage were also detected during the respective hours. The percentages of MII oocytes for both IVO and IVM groups were higher during 1200-1500 hours, which were 33.6±19.2% and 40.1±19.9%, respectively. In addition, high correlation values were obtained among the structures of IVM oocytes retrieved at the later hours (Appendix 3.5). The percentages of MII oocytes were not significantly different between the different retrieval hours of the day in both conditions. However, a significantly low MI (54.7±18.4%) was found at 1200-1500 hours *in vitro* as compared to early hours of oocyte retrieval (71.8±12.5%).

5.10.2.2 Structural appearance of IVO and IVM oocytes retrieved at the different times of the day post hCG injection

The percentages of MS, MTOC, NM and CG appearances in both IVO and IVM oocytes are summarised in Table 5.5. Significant variations ($p<0.05$) were detected in only MTOC and NM among the treatment groups. The values of MTOC (79.2±12.5%) and NM (97.5±2.5%) were significantly higher among IVO oocytes retrieved at 1200-1500 hours of the day. Comparatively, most of the structures were higher among IVO than IVM oocytes, except for the MS. This was especially so at 1200-1500 hours of retrieval time. The MS was highest at 0900-1100 hours of retrieval time (46.3±11.7%) in *in vitro* condition. The CG values were consistently higher at both retrieval times especially among the IVO oocytes and markedly reduced at 1200-1500 hours *in vitro*.

Table 5.5: Mean percentages of structural appearances in IVO and IVM of F_1 oocytes retrieved at the different hours of the day post-hCG injection

Treatment / Oocyte structure	IVO (%) (Mean ± SEM)		IVM (%) (Mean ± SEM)	
	0900-1100 hours	1200-1500 hours	0900-1100 hours	1200-1500 hours
MS	14.6±6.4[a] (n=41)	16.7±13.8[a] (n=10)	46.3±11.7[a] (n=58)	29.5±13.8[a] (n=27)
MTOC	41.9±11.5[a] (n=41)	79.2±12.5[b] (n=10)	26.4±9.1[a] (n=58)	61.7±12.2[a,b] (n=27)
NM	89.8±4.5[a,b] (n=51)	97.5±2.5[b] (n=28)	68.0±9.1[a] (n=71)	87.4±8.5[a,b] (n=36)
CG	100±0.0[a] (n=5)	100.0±0.0[a] (n=14)	88.6±8.6[a] (n=19)	65.0±11.3[a] (n=22)

[a,b] means in a row differ significantly at $p<0.05$.

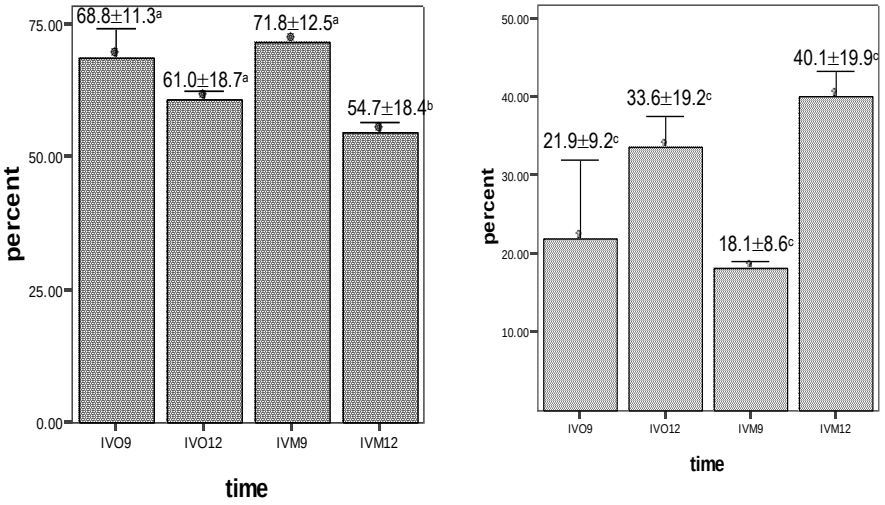

Figure 5.13: Average means of percentages of MI (left panel) and MII (right panel) oocytes retrieved at the different times of the day for both IVO and IVM conditions. [a,b,c] means within a group differ significantly at $p<0.05$.

5.10.3 Effect of Incubation Hours on Maturation Stages and Structural Appearance of IVM Oocyte.

In this experiment, oocytes from two strains of mice which were the F_1 and C57BL/6J were retrieved 13 hours post-hCG and cultured *in vitro*. The durations of incubation were 3 hours and 6 hours, respectively, for each group. The results entailing maturation stages and structural appearance of the oocytes are presented in Table 5.6. For 3 hours incubation, the percentages of MI and MII oocytes of C57BL/CJ were negatively correlated ($p<0.05$) as well as between the MII stage with the MS. The correlation values were r=-0.954 and r=-0.992, respectively. Its MS however, was positively correlated with MI stage (r=0.962). Among the F_1 oocytes, a negative correlation (r=-0.9720) was also determined between the MI and MII stages during 3 hours incubation *in vitro*. Meanwhile, among MII stage, positive correlations were found between MTOC and MS with CG, with r=0.634 and r=0.678, respectively. No correlation values were computed for 6 hours incubation due to small sample sizes in both strains.

The mean percentages of MII oocytes were found to be higher during 6 hours incubation in both strains. The values amounted to 40% for the F_1 and 30% for C57BL/6J oocytes. The MS and NM appearances were consistently high during both incubation hours with C57BL/6J oocytes outnumbered the MS of F_1's when almost all of the oocytes (100%) showed intact MS. It was 56% and 14%, respectively, of MS for 3 hours and 6 hours incubation for the later strain. The NM percentage was also higher during 6 hours incubation for both F_1 and C5BL/6J oocytes. The highest value was 93% of C57BL/6J oocytes. The MTOC of both strains were low in which less than 50% of the oocytes displayed the structure during both hours of incubation period.

Table 5.6: Mean percentages of maturation stages and oocyte structures in different incubation hours *in vitro* in two strains of mice

Category	Strain / Incubation hour			
	F_1		C57BL/6J	
	3 hours (% ± SEM)	6 hours (Mean %)	3 hours (% ± SEM)	6 hours (% ± SEM)
MI	74.5±9.9 (n=92)	57.9 (n=7)	75.7±6.6 (n=26)	67.4±20.2 (n=17)
MII	19.3±8.9 (n=92)	40.0 (n=7)	14.5±10.1 (n=26)	29.9±17.4 (n=17)
MS	55.6±9.2 (n=92)	14.3 (n=7)	75.0±20.5 (n=26)	100±0.0 (n=17)
MTOC	37.3±10.1 (n=92)	28.6 (n=7)	36.9±18.7 (n=26)	35.4±2.1 (n=17)
NM	67.3±5.6 (n=71)	89.0 (n=9)	82.1±9.0 (n=36)	92.9±7.2 (n=15)
CG	81.0±4.8 (n=52)	Not included	77.1±10.4 (n=11)	Not included

n=number of oocyte

5.10.4 Effects of Partial Zona Dissection on Oocyte Structures

The technique described by Nakagata (2000) was adopted to create a slit on zona layer of an oocyte as shown in Figure 5.14. Comparative morphology of the untreated (Figure 5.14a) and treated oocytes (Figure 5.14b,c) were shown. Observation revealed that oolemma of the PZD oocyte detached completely from zona, creating a wider gap occupying the vitelline space. The cytoplasmic appearance became unevenly distributed and engorged with dark spotty protuberances.

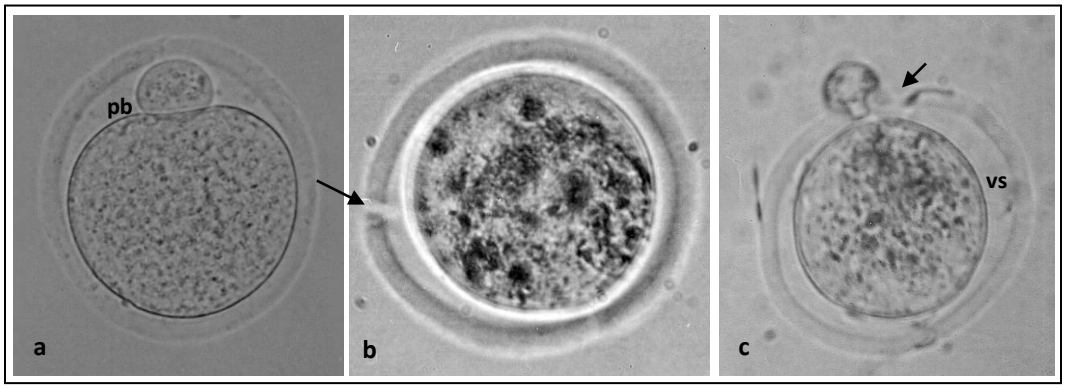

Figure 5.14. Bright-field images of a normal MII oocyte (a) and PZD oocytes (b) and (c). Arrows showing the slits made on the zona layer. pb-polar body, vs-peri-vitelline space. (400x)

Fluorescence staining of the MS, MTOC and NM revealed insignificant structural appearances between the treated and untreated oocytes in the three strains of mice. The mean percentages of each category were represented by the bar charts as displayed in Figure 5.15. Higher percentages of MS were comparatively observed in both of PZD oocytes of ICR (51.1±24.8%) and C57BL/6J (86.6±0.9%) than their IVM counterparts. The lowest MS value (14.3±14.3%) was detected in PZD oocytes of F_1. The NM in both of PZD and IVM oocytes were consistently high with the highest value detected in IVM oocytes of C57BL/6J and the lowest was among PZD oocytes of ICR. The respective values were 93.5±3.9% and 66.7±33.3%. Unlike the NM, the percentages of MTOC were comparatively lower in PZD than IVM oocytes. This was especially so in ICR mice when none of its oocytes showed MTOC structure. Low MTOC was similarly observed among PZD oocytes of both C57BL/6J and F_1, with values of 10.1±7.2% and 12.2±2.2%, respectively.

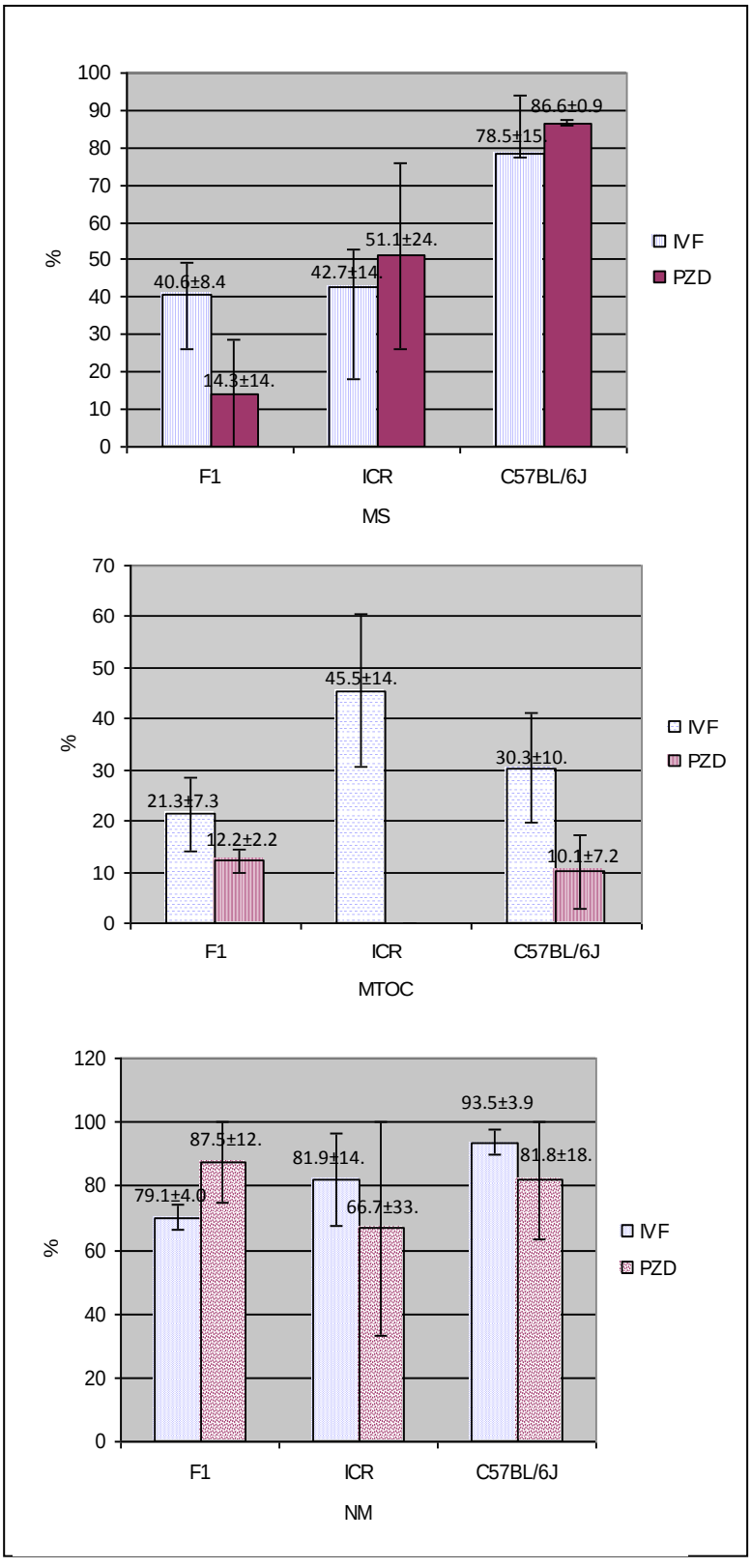

Figure 5.15: Mean percentages of MS (top), MTOC (middle) and NM (bottom) of PZD and IVM oocytes in three strains of mice.

5.11 DISCUSSION

The fate of mammalian oocytes relies greatly on its molecular machinery functions and interactions, which is manifested into structural appearance and functions. However, the developmental competency of oocytes varies due to external influences and manipulative environment. In this experiment, oocyte maturation stages and morphological appearance of selected structures namely MS, MTOC, NM and CG using ICC technique have been extensively described and compared between several treatments and strains of mice. Although the works depended mostly on conventional apparatus and instrumentations, nevertheless, the objectives of the experiment had been successfully accomplished revealing enormous findings on microscopic anatomy of the mouse oocytes. Using fluorescence staining technique, observation on temporal and spatial distribution of selected structures of oocytes had been successfully compared and elucidated. Comprehensive information from both the brightfield and the fluorescence images of the oocytes were collectively gathered to advance our understanding on structural organisation and factors affecting mammalian oocyte maturation. The objectives of the experiments; a) to compare structural appearance between MI and MII oocytes, b) to analyse structural development of oocyte in different maturation conditions, c) to identify structural differences of oocytes retrieved at different hours of the day and d) to determine the effect of mechanical stress such as partial zona dissection on oocyte structures.

In natural condition, mammalian oocytes which are quiescence at prophase I, resume its meiotic division to metaphase II at ovulation and eventually completing meiotic II only at time when it is triggered by sperm at fertilisation. A mature ovulated oocyte can be morphologically distinguished from immature ones by the presence of polar body. In laboratory environment, oocytes are produced in prodigious amount by the ovaries which

were administered through hormonal stimulation. Hence, the maturation stages of oocytes produced are vaguely defined and vary substantially in terms of its cytoplasmic and nuclear activities. However, the ICC technique adopted had provided satisfactory results on architectural topography for comparing the stages of maturation activities in mouse oocyte. Assessment on nuclear maturation was based on the organisation of the nuclear materials and meiotic spindles as described by Ibanez *et al.* (2005) and Hu *et al.* (2001). Meanwhile, distribution of cortical granules was used as the indication of cytoplasmic maturation (Liu *et al*., 2005). The oocytes prepared using ICC staining procedures were viewed and analysed using both brightfield light microscopy as well as the fluorescent optical imaging systems for describing the overall shape and identifying the distributions and locations of specific structures. This staining method has been preferably adopted in many laboratories in studying mammalian oocytes because of many reasons, among which are its high sensitivity and specificity (Vonesh *et al*., 2006) plus fascinating colourful images obtained. An additional advantage was that the prepared samples could be viewed via dual system though which more information and comparisons could be explored. The oocytes which appeared monotonous under the ordinary bright field light microscope (Figure 5.1a) demonstrated two distinguished regions when viewed under the red emission spectrum using the fluorescent microscope. A clear translucence space of the animal pole could be seen as compared with a darker vegetal pole (Figure 5.4a), which did not appear under the green emission filter (Figure 5.4b). This clearly defined the specific excitation property of the probe particles used for tagging the structures of an oocyte, hence, displaying the distribution of the identified structures. In addition to that, meiotic spindles and nuclear materials of the ICC prepared oocytes (Figure 5.3) were also clearly revealed under the brightfield images. This provides additional benefits of using the technique for easy

searching and locating the structures and most importantly to minimise bleaching effect due to long exposure of samples to the UV light. A smaller end of the animal pole where the meiotic spindles and nuclear materials were eccentrically assembled was void of granular materials in contrast to a broader vegetal pole with numerous aggregations of vesicular structures as seen in Figure 5.2. Segregation of oocyte structures that are associated with anterior-posterior positioning of an oocyte are determined by both genes and signals. Both of these elements have been successfully identified (Martin, *et al*., 2003). In relation to that, further studies could be conducted that include advanced search on signaling communication (Schubach, 2008) for regulating structural distribution associated with oocyte polarity. Variation in signaling pathways of oocyte amongst the strains and culture conditions are yet to be compared and resolved.

The general morphology and maturation stages of mouse oocytes have been extensively described (Schatten *et al*., 1992; Segers *et al*., 2008). These included the patterns of spindle appearance and nuclear maturation (Hu *et al*., 2001; Ibanez *et al*., 2005) and cortical granules distribution (Liu *et al*., 2005). Morphological observation revealed variation of shapes among the oocytes, most of which were round. Others have oval shape, potato shape and egg shape. It was difficult to correlate shape of oocytes with strains of mice. The images observed were also affected by the way oocytes were positioned onto coverslips. The use of a chambered glass slide is recommended in future microscopic analyses to avoid cell damage and cell loss. The spacer of the slide would ease the mounting process underneath the coverslip and may allow ones to observe intact live cells. Observation also revealed compartmentalised segments in some oocytes. This was especially so among the Alexa-flour®568 stained oocytes, which defined actin distribution. The similar segments were inconspicuously shown in oocyte stained with FITC-conjugated

anti-tubulin (Figure 5.9). The result not only characterised the distribution of actin but also its relationships with other structures of an oocyte. This unexceptional appearance of actin in MI oocyte might be correlated with its important role in aggregation of MTOC and movement of spindle to oocyte periphery (Calarco, 2005). In MII oocytes, actin concentrated mostly at the animal pole surrounding the polar body, revealing its role in cytokinesis. Actin has also been reported to be inseparable with cortical granules exocytosis (Wessels *et al*., 2002; Schietrome *et al*., 2007) and migration of nuclear materials to the periphery of the mammalian oocytes (Sun and Schatten, 2006). Actin distribution was briefly highlighted in this section because of several limitations among which was insufficient number of fluorescent filters to perform multiple staining. Due to that, ICC staining for actin was separately conducted on the different batches of oocytes. Consequently, it involved extra samples, time and energy inputs.

In this experiment, fluorescence images clearly distinguished immature from mature oocytes. This was achieved by assessing both its nuclear and cytoplasmic maturations. A prominent morphological comparison that distinguishes MI from MII oocytes is the appearance of a polar body in the later stage. Meanwhile, cellular responses to mark cytoplasmic maturation are relocation of organelles and exocytosis of the cortical granules (Liu *et al*., 2005). Although it is basically known that only a small percentage of mammalian oocytes would attain maturity, nevertheless, some variations were observed among the strains as well as between the culture conditions. Overall results showed less than 50% of oocytes attained MII stage in most strains and treatment groups in both *in vivo* and *in vitro* conditions. In general, *in vitro* culture had profoundly increased the number of mature oocytes. This was proven in ICR oocytes. In other strains such as the F_1 and C57BL/6 mice, longer exposure to *in vitro* culture had improved MII oocyte collection.

Among the three strains, C57BL/6 produced the highest percentage of MII oocytes *in vivo*. In F_1 mice, delaying the time for oocyte retrieval, the next day following hCG injection had increased the amount of IVO and IVM mature oocytes. This was in line with the finding in the human oocytes (Son *et al*., 2008). These results had proven the interplay of various factors that affect oocyte maturity. Also, susceptibility of oocytes to survive and mature in different environments might be influenced by many factors including genetic factors and culture conditions (Hafez, 1971; Liu *et al*., 2005 and Ibanez *et al*., 2005). Others could be the health status, age, nutrient and the housing condition of the female mice. Oocyte maturity depends greatly on cyclical accumulation of cyclin and cyclin-dependent kinase. Perhaps, inadequate supply and unequal distribution of such factors may have led to some oocytes having excessive amount at the expense of others, resulting in only a few being recruited to develop and mature. Besides, oestrus stage of the administered female mice may have also contributed to varying stages of nuclear and cytoplasmic maturity of oocytes as well as the oocyte sizes (Mrazek and Fulka, 2003). Exposure to *in vitro* environment may expose oocyte to reserve supply of nutrients and essential components to ensue maturity stage. In addition, low MII values probably resulted from several anomalies detected among the oocytes as shown in Figures 5.11a_2-d_2. Oocyte anomalies could provide some insights on structural incompetency in relation with failure of meiotic progression in *in vivo* and *in vitro* conditions, therefore, highlighting complexity of mammalian oocytes formation and development. Most mammalian oocytes are meiotically arrested at dictyate stage of prophase I and resume cell cycle progression to metaphase I only a few hours before ovulation *in vivo* (Johnson, 2007). However, hormonally induced animals may take 10-13 hours for ovulation to occur (Gates, 1971) and subsequently mature and arrested at metaphase II. Some differences of the MII values

obtained were statistically insignificant. This was probably due to small sample size included in the experiments.

A comprehensive result on oocyte structures was obtained by using multiple dyes staining technique. In comparing the oocyte structures among the strains of mice, F_1 usually possessed narrower and elongated meiotic spindles as compared with shorter, broader and compacted spindles in both the ICR and C57BL/6J oocytes. Different stages of spindle formation such as tangential and radial orientations represented MI and MII oocytes, respectively. There were also oocytes with intact spindles radiated poles to poles and some with incomplete arrays of unequal length and width of spindles. This reflected on the non-synchronous nuclear maturation probably due to unequal accumulation of maturation promoting factor. The microtubule organising centres were numerous in some and yet undetectable in others. The MI stage having full complement of chromosomes (2n=40) lacked polar body. They could be further described to bear tangentially positioned meiotic spindles, with cortical granules being either centrally located or highly accumulated at the bottom hemisphere of the vegetal pole. Meanwhile, chromosomes were arranged in rosette appearance at metaphase II stage and cortical granules were mostly abundant at the centre or vegetal hemisphere, unless activated; they were either sparsely distributed or aggregated at the peripheral region of the oocyte. Multitude of factors including both internal and external factors could have affected the complexity of structural distribution among the oocyte. Internal influence comprehends its genetic factors and natural surrounding that mediate oocyte meiotic machinery functions as opposed to external influence of *in vitro* environment. These were also previously reported (Bedford, 1971; Ibanez *et al*., 2005; Liu *et al*., 2005) for determining aged or mature oocytes. Oocytes, the mammalian female germ cells progress from immature (MI) to mature (MII) stage meiotically. Meiosis I stage

is crucially important in determining the formation of a normal and mature metaphase II oocyte, which could be clearly ascertained by the presence of a polar body resulting from the second meiotic division.

The results obtained from all three parts of experiments revealed that F_1 and C57BL/6J mice had high MII oocytes *in vivo*. These values indicated their IVO oocytes were more superior as compared to the IVM counterparts (Liu *et al*., 2005). Although general observation showed that ICR is the strain of choice to produce highly matured oocytes *in vitro*, however, cytoplasmic maturation competency among its IVM oocytes is impeded as shown by low cortical granules appearance as compared to other strains. Higher MII stage in ICR mice could have resulted from the effect of medium constituents, which had also caused *in vitro* activation of the oocytes. Perhaps, such process occurred at a slower rate in both F_1 and C57BL/6J, consequently resulting in the delay of cytoplasmic and nuclear maturation, hence, slowering the maturation process of the oocytes. This reaffirmed the statement that *in vitro* grown oocytes with oil overlay could delay meiotic progression (Segers *et al*., 2008). Activation of oocytes in *in vitro* environment might cause loss of cortical granules through exocytosis resulting in fertilisation failure (Miyara *et al*., 2003); a criterion to evaluate cytoplasmic maturation of oocytes (Damiani *et al*., 1996). Cytoplasmic maturation is essentially required for embryonic development *in vitro* (Elder and Dale, 2000), however, cortical reaction could release enzymes, which harden zona pellucida of an oocyte and consequently impeding fertilisation. This experiment proved that longer exposure to *in vitro* environment had induced high production of MII oocytes in F_1 and C57BL/6J mice. The two folds increased at 6 hours incubation as compared with 3 hours possibly prove the effect of oil overlay in delaying maturity among these oocytes. Although the results were insignificantly different between the culture hours the

result may provide some significant impacts on IVM or IVF practices and eventually its end results. Nowadays, many IVF procotols especially in mice commonly required 3 to 4 hours of *in vitro* insemination (Hogan, 1986; Jackson Laboratory, 2008; Elder and Dale, 2000) prior to *in vitro* culture. Accordingly, optimal insemination and maturation hours *in vitro* should be more specific among the strains due to their varied responses. This is in lined with many reports on the influence of genetic background (Polanski, 1986; Ibanez et al., 2005) and constituents of the culture medium (Liu *et al.,* 2005) on oocyte maturation and IVF. Moreover, *in vitro* maturation is known to alter the meiotic time course as reported by Segers *et al*. (2008). They found that oil overlay for *in vitro* prepared oocytes caused a differential hormonal exposure among *in vitro* grown mouse follicles by a differential segregation into the oil overlay. However, this did not impair the competence of cultured oocytes to proceed to MII, but delayed meiosis I progression. In ICR, relocation of cortical granules could have been related to *in vitro* exposure which induced oocyte meiotic progression from metaphase II to anaphase II and subsequently telophase II. Spontaneous activation of some mammalian oocytes has been reported once they were aspirated from mature follicles (Grondahl, 2008). Overall, oocyte maturation is a process that could arrest and resume in response to different stimuli (Persson *et al*., 2005).

Developmental competency of IVO and IVM oocytes depends upon synchronous maturation of both nuclear and cytoplasmic materials which are manifested by reorganisation of oocyte structures including chromosomal and meiotic spindles assembly and redistribution of vesicular structures such as cortical granules. A significantly high prevalence of meiotic spindles in *in vitro* condition was found among all strains of mice as compared with the IVO groups, especially in C57BL/6J oocytes. This was consistent with the earlier report (Ibanez *et al*., 2005) that the environment in which the oocyte undergoes

maturation is a critical factor in establishing and maintaining microtubule patterning in mouse oocytes. Moreover, high meiotic spindles occurrence in C57BL/6J oocytes was also observed during 6 hours of incubation periods as compared with the F_1 oocytes. Although genetic influence on superiority of strains to survive in *in vitro* condition has been clearly defined, however, factors that influenced C57BL/6J oocytes to produce a consistently high occurrence of the entire structures understudy in both IVO and IVM oocytes need further investigation. The IVM oocytes of F_1 showed low MII count, however, it was noted that its structural development was comparable with those of C57BL/6J except lower percentages of MS and NM. In addition, delaying the time of oocyte retrieval not only improved its survival *in vitro* but also consistently produced higher appearances of structural development especially MTOC and NM in both of the IVO and IVM oocytes. This was also proven by low correlation values obtained between oocyte maturity and structural appearance at the earlier hours of retrieval time than the later hours. This showed that structural development in F_1 oocytes was time dependence. Interestingly, it was reported by Son *et al*. (2008) that extending the period of hCG priming time from 35 to 38 hours for immature oocyte retrieval promotes oocyte maturation *in vivo* and increases the IVM rate of immature oocytes. Therefore, oocyte retrieval after 38 h of hCG priming may improve subsequent pregnancy outcome, in cycles programmed for IVM treatment. Although this indicate the optimal time of oocyte collection by referring to its nuclear maturation, however, the reduction in CG and MS appearance at 1200-1500 hours among the IVM group in F_1 oocyte, might hamper its fertilising competency. In addition to that, the CG was also vaguely correlated with other structures among the IVM oocytes as compared with the IVO counterparts. Since *in vitro* environment generally improved oocyte maturity, therefore oocyte collection time of the day for IVM and IVF applications

in mice prior to midday is highly encouraged to avoid spontaneous cytoplasmic aging. Oocyte collected later than the time may experience structural incompetency during prolonged *in vitro* exposure that consequently may affect IVF results.

Recent technology has developed various methods and devices to circumvent infertility. Micromanipulation technique usually requires oocyte to be handled with mechanical instruments such as micromanipulation needles. However, little information is available about its effects on oocyte structural developmental competency. In this experiment, PZD method has been utilised to impose mechanical stress through zona dissection and eventually exposed the oocyte contents to *in vitro* environment. There were insignificant variations with respect to MS, MTOC and NM appearances between the IVM and PZD oocytes. However, MS appearance in F_1 was lower as compared with ICR and C57BL/6J oocytes. Low MTOC and NM percentages were also observed in all the strains. Hence, F_1 oocytes could be more liable to experience structural impairment as compared with ICR and C57BL/6J. Strain superiority for manipulative application such as PZD was again shown by C57BL/6J oocytes based on its MS value and comparable results of MTOC and NM with the IVM group. Thus, strain selection is crucial for manipulation purpose in mouse oocytes. For example, many laboratories favour C57BL/6J as the experimental strain in IVF and transgenic research. In this part of the experiment, CG appearance was not detected due to various constraints especially sample size and technical problem. Analyses on CG appearance would be advantageous to study oocyte cytoplasmic maturation or aging among PZD oocytes. This may be paralleled with the results proposed by Sigurdson *et al*. (1992) that mechanical stress can initiate Ca wave and ATP release (Grygorzyk and Hanrahan, 1997; Yamamoto *et al*., 2000), which simulate the influence of sperm penetration at fertilisation process. The disadvantages of using PZD method were; a)

it may cause severe damage to oocytes with rigorous cut and b) lysis of cytosol due to osmotic influx of medium.

5.12 CONCLUSIONS

In conclusion, the experiments conducted provided archives of both brightfield and fluorescence images of the MI and MII oocytes. Comparative maturation stages were morphologically distinguished by the presence of polar body through bright-field observation. Meanwhile nuclear and cytoplasmic maturations were determined through ICC staining of the respective structures namely NM, MS and CG. Multiple staining of ICC technique produces more informative and comprehensive morphological appearances of the mouse oocytes. However, more structural analysis could be performed such as actin distribution, if adequate supply of fluorescent filters is to be installed in the existing system. Overall, the percentages of MII oocyte among the strains and treatment groups were low. However, variation in the results revealed the effects of the following factors in MII yields. Among all, C57BL/6J mice displayed strain superiority in both *in vivo* and *in vitro* environments. This was proven by its consistently high outputs of MII and structural appearances in both environments. The F_1 oocytes have proven to increase the production of MII stage in both IVO and IVM oocytes if retrieved at the later hours of the day following hCG injection. This explains the delay in maturation stages. Extending the time between hCG priming and oocyte collection has been associated with oocyte undergoing complete cellular and maturation processes, hence, improved survival and competency (Son *et al*., 2008). This was also emphasised by high correlation values among the structures obtained among the MII oocytes collected at a later time of the day. Meanwhile, *in vitro* environment has generally produced higher MII oocytes especially the ICR strain. Longer exposure to *in vitro* culture had also influenced MII production in both C57BL/6J and F_1

oocytes. Nevertheless, longer *in vitro* exposure had also resulted in cytoplasmic aging in the F_1 and ICR oocytes due to reduction of MS and CG appearance. Thus, the optimal hours of oocyte collection is recommended between 13-15 hours post hCG injection, to compromise the effect of *in vitro* activation and nuclear maturation. Structural anomalies detected among the oocytes, which have probably contributed to low count of MII were fragmented NM, disarrayed MS and patchy cytoplasm and CG. The effect of PZD dissection showed insignificant effect among the oocytes, especially C57BL/6J mice. Nevertheless, low appearance of MS and CG in PZD oocytes of F_1 mice has shown its lower competency for such treatment. The study had successfully identified some contributing factors, with regards to oocyte survival and competency in *in vivo* and *in vitro* environments that corresponded significantly with its structural developments. These findings could be useful as reference for future research in mammalian reproductive technology. Nevertheless, the application of advanced technique such as confocal imaging is recommended and could possibly provide more insights on oocyte structural development. Also, the use of chambered-slide is also proposed to ease staining steps when dealing with round cells such as mammalian oocytes.

REFERENCES

Abbott, A.L., Z. Xu, G. S. Kopf, T. Duibella and R.M. Schultz. 1998. *In vitro* culture retards spontaneous activation of cell cycle progression and cortical granule exocytosis that normally occur in *in vivo* unfertilised mouse eggs. Biology of Reproduction. 59(6):1515-1521.

Aktas, H., M.L. Lorainne and N.L. First. 2003. Meiotic state of bovine oocyte is regulated by interactions between cAMP, cumulus, and granulosa. Molecular Reproduction and Development. 65(3):336-343.

Bedford, J.M. 1971. Techniques and criteria used in the study of fertilisation. In: Methods in Mammalian Embryology. Freeman International Edition. 37-63.

Brunet, S., A.S. Maria, P. Guillaud, D. Dujardin, J.Z. Kubiak and B. Maro. 1999. Kinetochore fibres are not involved in the formation of the first meiotic spindle in mouse oocyte, but control the exit from the first meiotic M phase. Journal of Cell Biology. 146:1-11.

Byskov, A.G., C.Y. Anderson and L. Nordholm. 1995. Chemical structure of sterols that activate oocyte meiosis. Nature. 374:559-562.

Calarco, P.G. 2005. The role of microfilaments in early meiotic maturation of mouse oocyte. Microscopy and Microanalysis. 11:146-153.

Damiani, P., R.A. Fissore, J.B. Cibelli, C.R. Long, J.J. Balise, J.M. Robl and R.T. Duby. 1996. Evaluation of developmental competence, nuclear and ooplasmic maturation of calf oocyte. Molecular Reproduction and Development. 45:521-534.

Daniel, J.C. 1971. Methods in Mammalian Embryology. Freeman International Edition.

De Loos, F.A.M., E. Zeinstra and M.M. Bevers. 1994. Follicular wall maintains meiotic arrest in bovine oocyte cultured *in vitro*. Gamete Biology. (Abstract).

Downs, S.M., A.C. Schroeder and J.J. Eppig. 1986. Serum maintains the fertilising ability of mouse oocyte matured *in vitro* by preventing the hardening of the zona pellucida. Gamete Research. 15:115-122.

Ducibella, T. and J. Buetow. 1994. Competence to undergo normal, fertilisation-induced cortical activation develops after metaphase I of cAMP levels and cAMP phosphodiesterase activity. Developmental Biology. 165:95-104.

Ebner, T., M. Moser, C. Yamaan, O. Feichtinger, J. Harti and G. Tews. 1999. Elective transfer of embryos selected on the basis of the first polar morphology is associated with increased rates of implantation and pregnancy. Fertility and Sterility. 72:599-603.

Elder, K. and B. Dale. 2000. *In Vitro* Fertilisation. Second Edition. Cambridge University. 2-27.

Epigg, J.J. and A.C. Schroeder. 1989. Capacity of mouse oocyte from preantral follicles to undergo embryogenesis and development to live young after growth, maturation and fertilisation *in vitro*. Biology of Reproduction. 41(2):268-276.

Epigg, J.J., M. O'Brien and K. Wigglesworth. 1996. Mammalian oocyte growth and development *in vitro*. Molecular Reproduction and Development. 44:260-273.

Gates, A.H. 1971. Maximal yield and developmental uniformity of eggs. In: Methods in Mammalian Embryology. Freeman International Edition. 64-75.

Gobarsky, G.J., C. Simerly, G. Schatten and G.G. Borisy. 1990. Microtubule in the metaphase-arrested mouse oocyte turn over rapidly. Proceedings of the National Academy of Sciences USA. 87(16):6049-6053.

Grondahl, C., J.L. Otteson and M. Lessl. 1998. Meiosis-activating sterol promotes resumption of meiosis in mouse oocyte cultured *in vitro* in contrast to related oxysterols. Biology of Reproduction. 58:1297-1302.

Grondahl, C. 2008. Oocyte maturation. Danish Medical Bulletin. 55(1):1-16.

Grygorzyk, R. and J.W. Hanrahan. 1997. CFTR-independent ATP release from epithelial cells triggered by mechanical stimuli. American Journal of Physiology and Cell Physiology. 272: 1058-1066.

Hafez, E.S.E. 1971. Egg storage. In: Methods in Mammalian Embryology. Freeman International Edition. 117-132.

Hewitson, L.C, C.R. Simerly, M.W. Tengowski, P. Sutovsky, C.S. Navara, A.J. Haavisto and G. Schatten. 1996. Microtubule and chromatin configurations during rhesus intracytoplasmic sperm injection: successes and failures. Biology of Reproduction. 55: 271-280.

Hogan, B., F. Constantini and E. Lacy. 1986. Manipulating the Mouse Embryo: A Laboratory Manual. Cold Spring Harbor Laboratory, Cold Spring Harbor, NY, USA.

Hu, Y., I. Betzendahl, R. Cortvrind, J. Smitz and U. Eichenlaub-Ritter. 2001. Effects of low O_2 and ageing on spindles and chromosomes in mouse oocyte from preantral follicle culture. Human Reproduction. 16(4):737-748.

Ibanez, E., A. Sanfins, C.M.H. Combelles, E.W. Overstrom and D.F. Albertini. 2005. Genetic strain variations in the metaphase-II phenotype of mouse oocyte matured *in vivo* or *in vitro*. Reproduction. 130:845-855.

Jackson Laboratory. 2008. IVF protocol. Cryo.jax.org/ivf.html. Retrieved on June 23, 2008.

Johnson, H.M. 2007. Essential Reproduction. Sixth Edition. Blackwell Publishing. 185-186.

Kono, T., J. Carroll, K. Swann and D.G. Whittingham. 1995. Nuclei from fertilised mouse embryos have calcium-releasing activity. Development. 12:1123-1128.

Kubiak, J.Z., M. Weber, H. de Pennant, N.J. Winston and B. Maro. 1993. The metaphase II arrest in mouse oocyte is controlled through microtubule-dependent destruction of cyclin B in the presence of CSF. EMBO Journal 12:3773-3778.

Leader, B., H. Lim, M.J. Carabatsos, A. Harrington, J. Ecsedy, D. Pellman, R. Mass and P. Leder. 2002. Formin-2, polyploidy, hypofertility and positioning of the meiotic spindle in mouse oocyte. Biology of Reproduction. 61:1-7.

Lee, J. T. Miyano and R.M. Moor. 2000. Spindle formation and dynamics of γ-tubulin and nuclear mitotic apparatus protein distribution during meiosis in pig and mouse oocyte. Biology of Reproduction. 62:1184-1192.

Liu, J., A. Rybouchkin, J. Van der Eist and M. Dhont. 2003. Fertilisation of mouse oocyte from *in vitro* matured preantral follicles using classical *in vitro* fertilisation or intracytoplasmic sperm injection. Biology of Reproduction. 67(2):575-579.

Liu, X.Y., S.F. Mal, D.Q. Miao, D.J. Liu, S. Bao and J.H. Tan. 2005. Cortical granules behave differently in mouse oocyte martyred under different conditions. Human Reproduction. 20(12):3402-3413.

Martin, S.G., V. Leclerc, K. Smith-Litiere and D. St. Johnson. 2003. The identification of novel genes required for Drosophila anteroposterior axis formation in germline clone screen using GFP-Staufen. Development. 130:4201-4215.

Miyara, F., F.X. Aubriot, A. Glissant, C. Nathan, S. Douard, A. Stanovici, F. Herve, M. Dumont-hassan, A.LeMeur, P. Cohen-Bacrie and P. Debey. 2003. Multiparameter analysis of human oocyte at metaphase II stage after IVF failure in non-male infertility. Human Reproduction. 18:1494-1503.

Mrazek, M. and J. F. Jr. Navara. 1994. Failure of oocyte maturation. Possible mechanisms for oocyte maturation arrest. Human Reproduction. 18(1):2249-2252.

Nakagata, N. 2000. A Review. Mouse spermatozoa cryopreservation. Journal of Mammalian Ova Research. 17:1-8.

Navara, C.S., N.L. First and G. Schatten. 1994. Microtubules organisation in the cow during fertilisation, polyspermy, parthenogenesis and nuclear transfer. The role of the sperm aster. Developmental Biology. 162:29-40.

Navarro-Garcia, F., C. Sears, C. Eslava, A. Cravioto and J.P. Nataro. 1999. Cytoskeletal effects induced by pet, the serine protease enterotoxin of enteroaggregative *Escherichia coli* . Infection and Immunity. 67(5):2184-2192.

Navarro, P.A., L. Liu, J.R. Trimachi and A.R. Ferriani. 2005. Non-invasive imaging of spindle dynamics during mammalian oocyte activation. Fertility and Sterility. 83(1):1197-1205.

Persson, J.L., Q. Zhang, X.Y. Wang, S.E. Ravnik, S. Muhirad and D.J. Wolgemuth. 2005. Distinct roles for the mammalian A-type cyclins during oogenesis. Reproduction. 130: 411-422.

Polanski, Z. 1986. *In-vivo* and *in-vitro* maturation rates of oocyte from two strains of mice. Journal of Reproduction and Fertility. 78:103-109.

Schatten, G., C. Simerly and H. Schatten. 1985. Microtubule configurations during fertilisation, mitosis, and early development in the mouse and the requirement for egg microtubule-mediated motility during mammalian fertilisation. Proceedings of the National Academy of Sciences USA. 82:4152–4156.

Schatten, H. and G. Schatten. 1986. Motility and centrosomal organisation during sea urchin and mouse fertilisation. Cell Motility and Cytoskeleton. 6:163-175.

Schatten, G., C. Simerly and H. Schatten. 1991. Maternal inheritance of centrosomes in mammals? Studies on parthenogenesis and polyspermy in mice. Proceedings of the National Academy of Sciences USA. 88:6785-6789.

Schatten, H., M. Walter, H. Biessmann and G. Schatten. 1992. Activation of maternal centrosomes in unfertilised sea urchin eggs. Cell Motility and Cytoskeleton. 23:61-70.

Schatten, G.1994. The centrosome and its mode of inheritance: The reduction of the centrosome during gametogenesis and its restoration during fertilisation. Developmental Biology. 165:299-335.

Schietrome, C. H.Y. Yu, M.C. Wagner, J.A. Umbach, W.M. Bemen and C.B. Gundersen. 2007. A role for myosin in cortical granule exocytosis in *Xenopus* oocyte. Journal of Biological Chemistry. 282:29504-29513.

Schultz, R.M., S. Kurasawa, Y. Endo and G.S. Kopf. 1989. Molecular events pre- and post-fertilisation of mouse eggs. Oocyte maturation, egg activation and polyspermy block. In: Medically Assisted Conception: Agenda for Research. National Academy Press. Washington DC.

Schubach, T. 2008. Establishment of asymmetries during *Drosophila* oogenesis. Research Abstract. Howard Hughes Medical Institute.

Segers, I., T. Adriaenssens, W. Coucke, R. Cortvrindt and J. Smitz. 2008. Timing of nuclear maturation and postovulatory aging in oocyte of *in vitro* grown mouse follicles with or without oil overlay. Biology of Reproduction. 78:839-868.

Simerly, C. and G. Schatten. 1993. Techniques for localisation of specific molecules in oocyte and embryos. Methods in Enzymology. 225:516-553.

Sigurdson, W., A. Ruknudin and F. Sachs. 1992. Calcium imaging of mechanically induced fluxes in tissue-cultured chick heart. Role of stretch activated ion channels. American Journal of Physiology: Heart Circulation Physiology. 262:1110-1115.

Sirad, M.A. and P. Blondin. 1996. Oocyte maturation and IVF in cattle. Animal Reproduction Science, Elsevier. 42:417-426.

Son, W.Y., J.T. Chung, R.C. Chian, B. Herrero, E. Demirtas, S. Elizur, Y. Gidoni, C. Sylvestre, N. Dean and S.L. Tan. 2008. A 38 h interval between hCG priming and oocyte retrieval increases *in vivo* and *in vitro* oocyte maturation rate in programmed IVM cycles. Human Reproduction. 23(9):2010-2016.

Sun, Q.Y. and H. Schatten. 2006. Regulation of dynamic events by microfilaments during oocyte maturation and fertilisation. Reproduction. 131:93-205.

Sorenson, R.A. and P.M. Wassarman. 1976. Relationship between growth and meiotic maturation of the mouse oocyte. Developmental Biology. 50(2):(Abstract).

Suppinyopong, S., R. Choavaratana and C. Karavakul. 2000. Correlation of oocyte morphology with fertilisation rate and embryo quality after intracytoplasmic sperm injection. Journal of Medical Association, Thai. 83:627-632.

Tateno, H., and Y. Kamiguchi. 2007. Evaluation of chromosomal risk following intracytoplasmic sperm injection in the mouse. Biology of Reproduction. Retrieved on April 4, 2007 as DOI:10.1095/biolreprod.106.057778.

Veselska, R. and R. Janish. 2001. Cortical actin cytoskeleton in human oocyte: a comparison with mouse oocyte. Scripta Medica. 74(4):265-274.

Vonesh, C., F. Aguet, J.L. Vonesh and M. Unser. 2006. The colored revolution of bioimaging. IEEE Signal Processing Magazine. 3(23):20-31.

Wessel, G.M., S.D. Corner and L. Berg. 2002. Cortical granule translocation is microfilament mediated and linked to meiotic maturation in the sea urchin oocyte. Development. 129:4315-4325.

Yamamoto, K., R. Korenaga, A. Kamiya and J. Ando. 2000. Fluid shear stress activates Ca influx into human endothelial cells via P2X4purinoceptors. Circulation Research. 87: 385-391.